Chapter 10
PhenoSat – A Tool for Remote Sensing Based Analysis of Vegetation Dynamics

Arlete Rodrigues, André R. S. Marcal, and Mário Cunha

Abstract PhenoSat is a software tool that extracts phenological information from satellite based vegetation index time-series. This chapter presents PhenoSat and tests its main characteristics and functionalities using a multi-year experiment and different vegetation types – vineyard and semi-natural meadows. Three important features were analyzed: (1) the extraction of phenological information for the main growing season, (2) detection and estimation of double growth season parameters, and (3) the advantages of selecting a sub-temporal region of interest. Temporal NDVI satellite data from SPOT VEGETATION and NOAA AVHRR were used. Six fitting methods were applied to filter the satellite noise data: cubic splines, piecewise-logistic, Gaussian models, Fourier series, polynomial curve-fitting and Savitzky-Golay. PhenoSat showed to be capable to extract phenological information consistent with reference measurements, presenting in some cases correlations above 70 % ($n = 10$; $p \leq 0.012$). The start of in-season regrowth in semi-natural meadows was detected with a precision lower than 10-days. The selection of a temporal region of interest, improve the fitting process (R-square increased from 0.596 to 0.997). This improvement detected more accurately the maximum vegetation development and provided more reliable results. PhenoSat showed to be capable to adapt to different vegetation types, and different satellite data sources, proving to be a useful tool to extract metrics related with vegetation dynamics.

A. Rodrigues (✉) • M. Cunha
Faculdade de Ciências da Universidade do Porto, Department of GAOT & Centro de Investigação em Ciências Geo-Espaciais, Universidade do Porto, Porto, Portugal
e-mail: dr.arlete@gmail.com; mcunha@mail.icav.iup.pt

A.R.S. Marcal
Faculdade de Ciências da Universidade do Porto, Department of Matemática & INESC TEC, Universidade do Porto, Porto, Portugal
e-mail: andre.marcal@fc.up.pt

Y. Ban (ed.), *Multitemporal Remote Sensing*, Remote Sensing and Digital Image Processing 20, DOI 10.1007/978-3-319-47037-5_10

10.1 Introduction

Temporal vegetation profiles based on remotely sensed data provide valuable information for understanding land cover dynamics, generally interpreted by vegetation phenological events. Sensors such as the Advanced Very High Resolution Radiometer (AVHRR), SPOT VEGETATION (Satellite Pour l' Observation de la Terre – Vegetation), MODIS (Moderate-Resolution Imaging Spectroradiometer), MERIS (Medium Resolution Imaging Spectrometer) and PROBA-V (Project for On-Board Autonomy – Vegetation) are able to provide a spatial overview of the land surface and spectral reflection information, which can be measured and used to monitor phenology, stage type and crops health (pionnering studies were made by Allen et al. 1969, 1973; Gausman et al. 1969, 1974; Wooley 1971; Gausman and Allen 1973; Gausman and Hart 1974). Furthermore, their ability to collect imagery at frequent time intervals (multitemporal images) permits to observe how the vegetation changes throughout the growing season and better monitor the changes naturally occurred or induced by humans.

Vegetation phenology based on remote sensing data refers to the spatio-temporal development of the vegetated land surface as revealed by satellite sensors (de Beurs and Henebry 2004). The main assumption behind all methods for phenological determination from satellite sensor data is that the signal is related to measures of vegetation. A time-series of a given vegetation index (VI) follows annual cycles of growth and decline. Thus, deriving phenological metrics from remotely sensed data consists on the analysis of the seasonal VI trajectory, and identifying critical points such as the start-of-season or the end-of-season (Bradley and Mustard 2008).

Although the access to Earth Observation Satellite VI time-series is cur-rently widespread, with low or without costs, there is still a gap between the data itself and the meaningful information that can be extracted. Phenological metrics exploit the seasonal growth cycle information, which could be influenced by non-climatic factors, biogenic and anthropogenic disturbances (fires, land degradation, insect attacks), or temperature and rainfall variations (Julien and Sobrino 2009; Potter et al. 2003). The large amounts of data and the presence of noise can make the analysis and extraction of relevant vegetation information a difficult and time consuming process.

The Maximum Value Composites (MVC) process is generally used to minimize the noise influence by analyzing the VI values on a pixel-by-pixel basis, in a predefined time-period, retaining the highest value for each pixel location (Holben 2007). A MVC image is obtained when all pixels have been evaluated. The MVC imagery is highly related to the green vegetation dy-namics, and common problems encountered in single-date remote sensing studies, as cloud contamination, atmospheric attenuation and observation geometry are minimized using MVC (Tucker et al. 1985). However, generally the MVC process is not sufficient to eliminate all unrealistic variability from VI time-series (Jonsson and Eklundh 2004; Rodrigues et al. 2013). Further-more, additional noise may be also introduced by the process of overlaying several images (for example due to image

Table 10.1 Filtering methods proposed for smoothing remotely sensed time-series of vegetation indices

Filtering method	Some prominent applications
Running medians	Velleman (1980)
Best index slope extraction	Viovy et al. (1992) and Lovell and Graetz (2001)
Weighted least squares windowed regression	Sweets et al. (1999)
Harmonic series and higher order splines	Roerink et al. (2000), McCloy and Lucht (2004) and Bradley et al. (2007)
Wavelets	Li and Kafatos (2000) and Sakamoto et al. (2005)
Asymmetric Gaussian	Jonsson and Eklundh (2002)
Double logistic	Zhang et al. (2003) and Beck et al. (2006)
Savitzky-Golay	Chen et al. (2004)
Mean value iteration	Ma and Veroustraete (2006)
Whittaker smoother	Atzberger and Rembold (2009) and Atzberger and Eilers (2010)
Breaks for additive seasonal and trend	Verbesselt et al. (2010)
Frequency analysis	Lhermitte et al. (2011)
Adaptive local iterative logistic fitting	Cao et al. (2015)

misregistration). Thus, it is necessary to fit a model to the observed data before the extraction of vegetation dynamics information. An appropriate model should be capable of smoothing the data without introducing artifacts or suppressing natural variations of the vegetation (Fontana et al. 2008). During the last years, different filtering techniques have been proposed (summarized in Table 10.1). In general, data smoothing facilitates the satellite time-series analyses, by eliminating the unrealistic abrupt peaks and aberrant values that appears in the VI profile (Fontana et al. 2008). Moreover, it permits a better observation of the vegetation changes over time and the identification of the main and double growing seasons, which is not always clearly possible using the VI original data. This is illustrated in the example presented in Fig. 10.1.

Developing algorithms to automatically remove the time-series noise and retrieve land surface phenology metrics from satellite data has been an active research topic for the last decade. TIMESAT (Jonsson and Eklundh 2004) is the most known software for time-series phenology analysis, being used in several research studies (e.g. Gao et al. 2008; Verbesselt et al. 2012; Zeng et al. 2013). It is an open source software and provides three different smoothing functions to fit the time-series data: asymmetric Gaussian, double logistic and adaptive Savitzky-Golay filter. TIMESAT uses a simple method, based on thresholds, to determine a set of phenological metrics, including the start-of-season, mid-season and end-of-season.

Besides TIMESAT, there are other software packages allowing the analysis of the satellite time-series, reduction of noise components and/or extraction of phenological metrics from satellite time-series data. HANTS (Roerink et al. 2000),

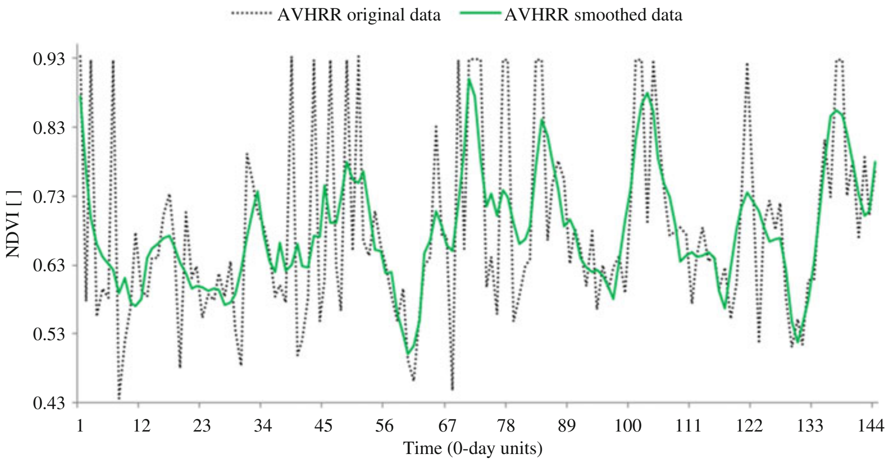

Fig. 10.1 Example of a temporal series of NDVI acquired from NOAA AVHRR for a semi-natural meadows region in Montalegre (Portugal) between 2001 and 2004. The *dotted black line* corresponds to the original NDVI data and the *solid green line* the smoothed data produced using the Savitzky-Golay method

TiSeG (Colditz et al. 2008), TSPT (Prados et al. 2006; McKellip et al. 2008), PPET (McKellip et al. 2010), TIMESTATS (Udelhoven 2011), the software developed by USGS Earth Resources Observation and Science Center (Ross et al. 2009), Enhanced TIMESAT (Tan et al. 2011) and the SPIRITS (Eerens et al. 2014) are some examples. Although these software products have important functionalities for the extraction of phenological information, they present two great limitations: (i) none of them allows the selection of an in-season window of interest, which is fundamental for analyzing vegetation types and crop systems with more than one growth cycle through the year; and (ii) except for TIMESAT, none of them has a specific option to characterize a double growth season phenology. Moreover, they work well in ecosystems with predictable minimum and maximum VI values, however they cannot adapt so well to different vegetation dynamics over the years, caused by uncontrollable conditions (drought year, unseasonal snow, fire, plagues and diseases), and crops with partial ground cover or period of dormancy.

To address the aforementioned limitations, PhenoSat was developed to detect the number of growth seasons in each year and has the option to define an in-season window of interest. The ability to model more than one growing season makes PhenoSat an useful tool for study different crops, able to deal with adverse weather and soil conditions. The main characteristics and functionalities of PhenoSat were tested using a multi-year experiment and different vegetation types, as well as data from two different sensors.

10.2 PhenoSat Description

PhenoSat is a software tool developed to extract phenological information from satellite VI time-series. This tool was implemented in Matlab (Higham and Higham 2000) using a simple interface to provide an easy-to-use soft-ware. PhenoSat can receive two standard input text files: containing the orig-inal satellite VI images, or containing a temporal VI dataset. For the VI im-ages, a pixel-by-pixel approach is conducted, and a specific region can be selected instead of using all image size. For a temporal dataset, the numerical values (VI) are already standardized in a text file.

A number of satellite based metrics related with main growing season phe-nological parameters (e.g. start-of-season, maximum vegetation develop-ment, end-of-season) can be determined by PhenoSat. Some vegetation types and crops systems present more than one growth cycle through the year manly related with crop rotation or vegetation regrowth. The timing and magnitude of these in-season cycles present high intra-annual variability due to some factors such as climate, animal grazing and human land use decisions. Information about the timing of start and maximum of these seasonal cycles can be obtained using PhenoSat. It is important to note that some extreme conditions (e.g. fire, unseasonal snow) could result in a false report of a double growing season. For this reason, a new feature was developed in PhenoSat that allows the selection of a sub-temporal region of interest, based on vegetation dynamics knowledge. The annual VI time-series subinterval, defined manually or automatically, improves the fitting process, providing more realistic results of the vegetation dynamics.

PhenoSat outputs two files containing the phenological information (es-timated date and respective VI value) and the processed data at each of the fitting steps. When the VI images are used as input, three additional output images will be created. These images present, for each pixel analyzed, the phenological estimated dates for three main stages: start-of-season, maximum vegetation development and end-of-season.

10.2.1 PhenoSat Fitting Methods

Some VI datasets available online from different sensors (e.g. AVHRR, SPOT VEGETATION (SPOT_VGT), MODIS) are already preprocessed in order to reduce the noise caused by a variety of biophysical factors (Carreiras et al. 2003; Gutman 1991; Li and Strahler 1992). Although this preprocessing is generally effective, the VI datasets still retain some problems (punctual outliers or abrupt changes) that require additional processing. Noise reduction filters can be applied to remove the undesirable artifacts, improving the subsequent analysis, and leading to more reliable vegetation dynamics information.

PhenoSat analyses year-by-year and considers as outliers the VI values that present a VI difference above 0.2 from the median (Mw), and from its left and right spatial neighbors. A VI profile variation of more than 0.2 is considered a high variation (abrupt increase or decrease) which is unexpected between consecutive observations in any vegetative crop cycle. The values of these outliers are replaced by the Mw value. To modify the bias of the fit, an upper envelope (Beck et al. 2006) can be applied. The upper envelope compares the smoothed and original data, and the data points below the model function are considered to be less important. This method enhances the spring and summer periods, allowing a better discrimination of the maximum vegetation development. Although these actions can remove the VI time-series outliers, some noise might still remain. For this reason, PhenoSat provides six methods that can be used to obtain improvements in the noise reduction process. The methods are: cubic smoothing splines (CSS), piecewise-logistic (PL), Gaussian models (GM), Fourier series (FS), polynomial curve-fitting (PCF) and Savitzky-Golay (SG). The CSS algorithm (Reinsch 1967) fits a cubic smoothing spline to the VI time-series data. The adherence of the smoothing spline method to the given data depends on the algorithm parameter selected.

Beck et al. (2006) and Fontana et al. (2008) proved that vegetation dynamics tends to follow a well-defined growth temporal pattern and the vegetation cycle can be represented by a double-logistic function. PhenoSat uses a particular case of a double-logistic function (PL) defined by Eq. 16.1, where t represents the time, VI_t the VI value at time t, c and d are the slopes at the 'left' and the 'right', and p and e are the inflection points dates. VI_w and VI_{w1} are the VI values before the bud break and after the leaf fall, respectively. The k parameter is related with the asymptotical value and assures the continuity between vegetation growth and senescence parts, even when they differ in shape (Cunha et al. 2010). The PL seven parameters are estimated using the Levenberg-Marquardt algorithm (Montgomery et al. 2006), which requires reasonable initial values.

$$VI_t = VI_w + \frac{k}{1 + \exp\left[-c\,(t-p)\right]} - \frac{k + VI_w - VI_{w1}}{1 + \exp\left[-d\,(t-e)\right]} \tag{10.1}$$

Figure 10.2 presents a representation of the PL parameters, using two consecutive years of NDVI (Normalized Difference Vegetation Index) SPOT_VGT data. The continuity between the 2 years is assured by the VI_w and VI_{w1}, being the VI_w for the second year (beginning of the time-series) the same as the VI_{w1} for the first year (final of the time-series).

The GM adjustment to data is given by the Eq. 16.2 (Goshtasby and Oneill 1994):

$$y = \sum\nolimits_{i=1}^{n} a_i e^{\left[-\left(\frac{x-b_i}{c_i}\right)^2\right]} \tag{10.2}$$

where a is the amplitude, b the centroid (location), c is related to the peak width and n is the number of peaks to fit ($1 \le n \le 8$).

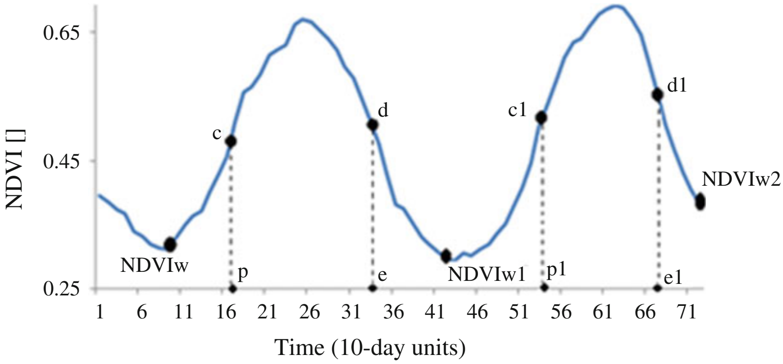

Fig. 10.2 Representation of the piecewise-logistic function parameters, using NDVI SPOT VEGETATION data from two consecutive years

The FS is a sum of sine and cosine functions of different period that describes a periodic signal (Mitra 2010). In the trigonometric form, it is represented as:

$$y = a_0 + \sum\nolimits_{i=1}^{n} [a_i \cos(nwx) + b_i \sin(nwx)] \tag{10.3}$$

where a_0 models a constant (intercept) term in the data and is associated with the $i = 0$ cosine term, w is the fundamental frequency of the signal, and n is the number of terms (harmonics) in the series ($1 \leq n \leq 8$).

The PCF (Verschelde 2007) finds the coefficients of a polynomial, of a given degree, that fits the data. The higher the degree, the closer the fitting curve will be to the data, although this should be done only up to a certain (reasonable) degree.

The SG filter (Press et al. 2007) defined by

$$g_i = \sum\nolimits_{nL}^{nR} c_n f_i + n \tag{10.4}$$

is a particular type of low-pass filter, that replaces each data value f_i, $i = 1, \ldots, N$, by a linear combination g_i of nearby values in a window defined by the number of points ‘to the left’ (nL) and ‘to the right’ (nR) of a data point i. In PhenoSat, the SG filter uses $nL = nR$ and is always applied to smooth the original VI data. For the subsequent analysis, it can be used alone or combined with one of the other methods.

Figure 10.3 presents a comparison of the six fitting methods described, using a NDVI SPOT_VGT annual time-series obtained from a Closed Deciduous Forest. The PCF and GM methods present the most distinct fitting results for the main and double growing seasons. The biggest differences are on the double growth season, where these two methods present low sensitivity to detect the regrowth peak, over smoothing this occurrence. It is important to note that PCF, GM, FS and CSS require a smoothing parameter to fit the da-ta. The results presented were obtained using an

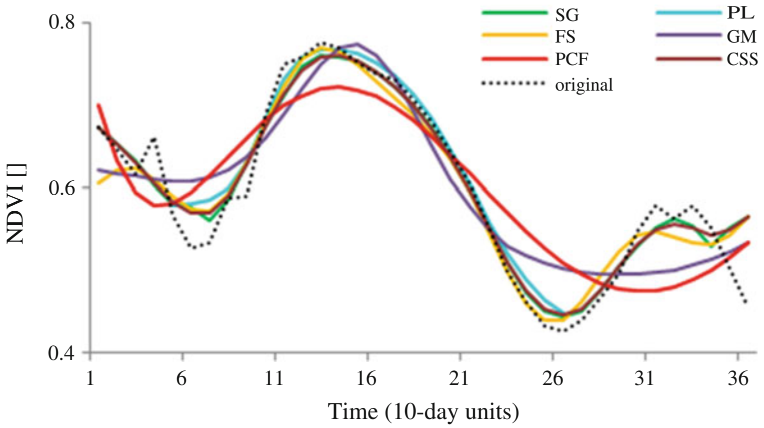

Fig. 10.3 Comparison of PhenoSat fitting methods using a NDVI SPOT VEGETATION annual time-series obtained from a Closed Deciduous Forest

intermediate value for each method in order to provide a more coherent comparison (a parameter of 5 was used in FS, GM and PCF methods, and a value of 0.5 for CSS).

10.2.2 Phenological Metrics

PhenoSat is able to determine the VI value and time of occurrence of the following seven phenological events in the main growing season: start-of-season (SOS), maturity (MAT- beginning of the ripening stage/full canopy), maximum vegetation development (MVD), senescence (SEN), end-of-season (EOS), and the maximum growth and maximum senescence rates (namely left (LIP) and right (RIP) inflexion points, respectively).

The phenological information is obtained using the derivatives of the fitting VI time-series, as illustrated in Fig. 10.4. The LIP (and RIP) corresponds to the maximum (and minimum) of the fitted first derivative. The MVD is determined as the maximum VI fitted value in the interval defined by LIP and RIP. The maxima of the fitted VI time-series second derivative, at the left/right of the MVD, identify the SOS/EOS. Similarly, the MAT/SEN can be found using the minima of the fitted data second derivative, at the left/right of the MVD.

Some factors, such as adverse weather conditions (snow, ice or extreme heat), water availability, pasture management and/or herbaceous vegetation growth in the winter season, can interrupt the first growth vegetation cycle and induce an annual regrowth in some crops (e.g. crop systems with more than one growth cycle a year, shrublands or semi-natural meadows). This phenological information can also be extracted by PhenoSat if required. This option allows recording the VI value and

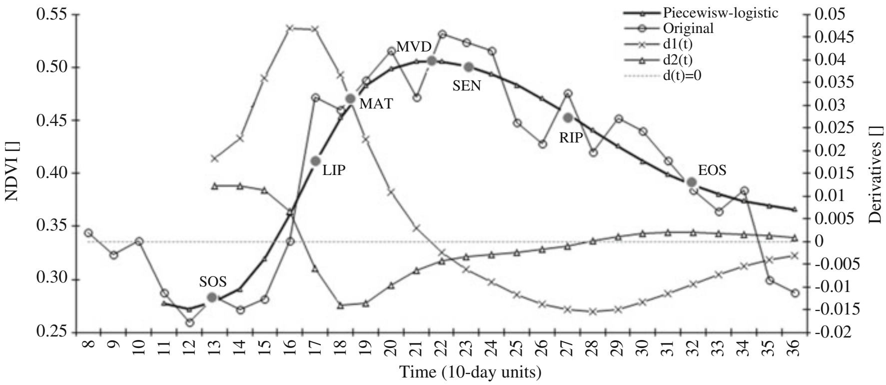

Fig. 10.4 Representation of PhenoSat derived phenological stages using the maxima and minima of the first and second derivatives of the NDVI fitted data

date of occurrence for the start and maximum of this in-season period. PhenoSat calculates the regrowth parameters using the pre- smoothed time-series (removed outliers and SG filter application) after the EOS time occurrence.

The regrowth start is defined as the point where an increase of three or more points occurs after the EOS stage. After this starting point, a decreasing period of two or more points determines the maximum of the regrowth. In some cases, the regrowth reported can be a "false regrowth". For example in vineyards, as many other discontinuous canopies, during the winter season the inter-row vegetation growth appears as a regrowth in the vineyard annual profile. The unseasonal snow could also result in a false report of a double growth season in many environments. Only with the knowledge/analysis of the ground conditions it is possible to infer about the truth of the regrowth.

The selection of an in-season temporal region of interest, based on known vegetation dynamics, can help dealing with a false regrowth, particularly for natural land cover types. PhenoSat has the possibility to select, automatically or manually, the in-season temporal region of interest. The manual selection can be done by inputting the initial and final time positions, based on known behavior of the vegetation in the field at normal growth conditions. This type of selection presents some limitations when adapting to different dynamics over the years. PhenoSat tries to solve this problem with an optional approach that automatically detects the region of interest. This option, based on the VI time-series profiles, is more flexible and can adapt to the dynamics variations over the years. To determine the annual time-series subinterval, PhenoSat firstly calculates the maximum value of the VI unfitted data. Then, searches for the initial position, which corresponds to the point where a significant increase (or abrupt decrease) is verified to the left of the maximum. Afterwards, to determine the final position, the algorithm proceeds in a similar way but evaluating the data to the right of the maximum.

10.3 PhenoSat Application

10.3.1 Study Area and Satellite Data

The PhenoSat software was tested for different vegetation types and geographical locations in continental Portugal. The NDVI time-series from AVHRR (10-days composite and 1-km resolution) and SPOT_VGT (10-days composite and 1-km resolution) covering Portugal, were downloaded from The Joint Research Centre Community Image Data portal (JRC-CID 2013).

The performances of PhenoSat were tested in two land use types that present, mainly, a different annual growth pattern (Table 10.2): vineyard (VIN) in Douro wine region (Northeast Portugal); and semi-natural meadows (SNM) in Montalegre (Northeast Portugal). In Douro region the predominant land cover is the vineyard with extensive contiguous areas. The vineyard has a long dormancy period with intense understory vegetation growth and a discontinuous canopy (Cunha et al. 2010). The SNM are an essential element of the mountain landscapes in Northern Portugal, and represent the main fodder resource for livestock production. This type of crop is characterized by a regrowth around the month of August, whose intensity and date of occurrence are mainly dependent of climatic conditions (Pocas et al. 2012).

The different vegetation profiles provided by these crops (Fig. 10.5) permit to evaluate the adaptability and performance of PhenoSat to distinct situations. For each crop, a training area was defined carefully to avoid pixel boundaries with other crops, hence the reduced number of pixels (Table 10.2) used in these experiments. Entire training areas were considered as units, instead of using a pixel-by-pixel approach. The median of the NDVI values of the pixels assigned to each crop

Table 10.2 Description of training areas and satellite datasets used to test PhenoSat

Land cover	Acronym	Coordinates (Long/Lat WGS84)	Satellite products	Time-series period	Size (pixels)
Vineyard[a]	VIN	UL: 7d45’17.7W, 41d09’51.6N	SPOT_VGT AVHRR	2001–2010	6
		BR: 7d43’41.8W, 41d08’48.4N			
Semi-natural meadows	SNM	UL: 7d57’36.9W, 41d38’15.2N	SPOT_VGT AVHRR	2001–2010	4
		BR: 7d56’33.4W, 41d37’11.6N			

[a]phenological field measures available
UL upper left corner, *BR* bottom right corner

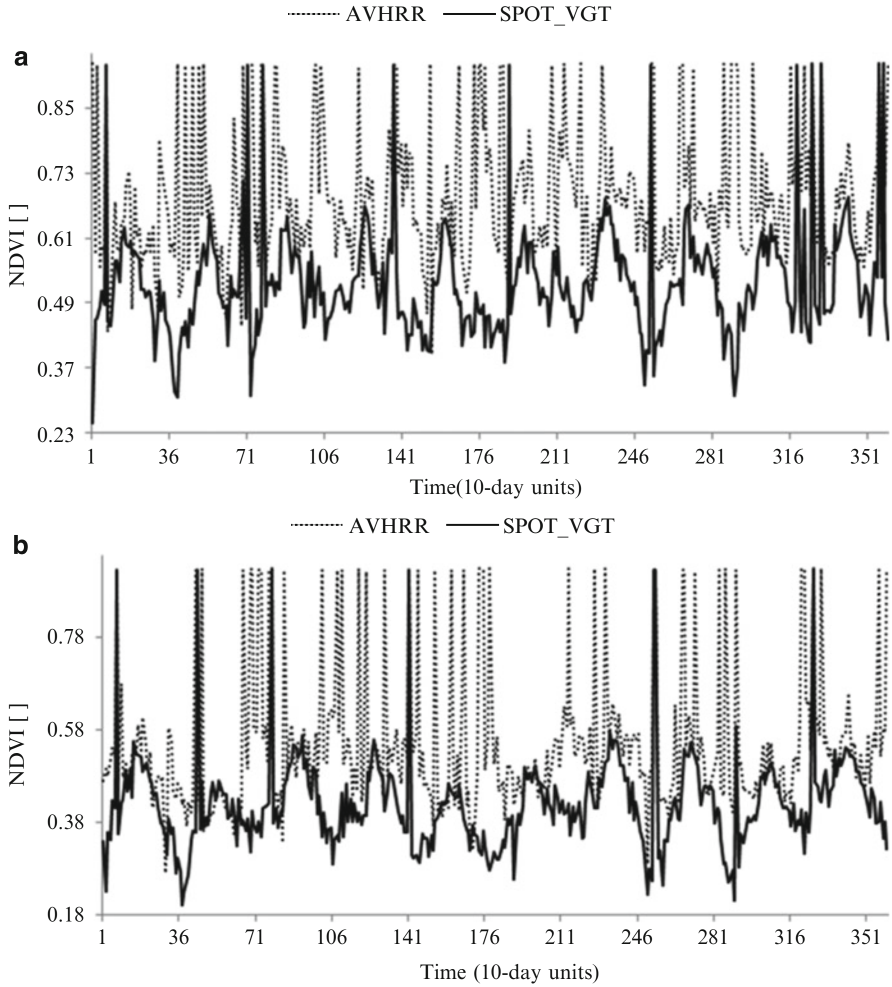

Fig. 10.5 Original NDVI temporal profiles obtained from SPOT VEGETATION and AVHRR data, for the semi-natural meadows (**a**) and vineyard (**b**) land use types, for the period 2001–2010

were computed. The yearly NDVI time-series were created using the median values obtained for each of the images available in a year.

10.3.2 Extraction of Phenological Information

The ability of PhenoSat to estimate phenological metrics from satellite VI data was evaluated by a comparison between PhenoSat derived phenology and reference

Table 10.3 Statistics of reference phenological measures obtained for vineyard (VIN) and semi-natural meadows (SNM) vegetation types

Phenological stage	Statistics	VIN	SNM
Start-of-Season	Mean (DOY)	82.16	98.00
	Maximum (DOY)	92.00	150.00
	Minimum (DOY)	78.00	70.00
	Standard deviation (days)	4.73	23.15
Flowering	Mean (DOY)	145.76	n.a.
	Maximum (DOY)	153.00	n.a.
	Minimum (DOY)	125.30	n.a.
	Standard deviation (days)	7.18	n.a.
Veraison/Maximum Vegetation Development	Mean (DOY)	204.20	169.00
	Maximum (DOY)	213.50	180.00
	Minimum (DOY)	199.70	150.00
	Standard deviation (days)	4.07	10.44
End-of-season	Mean (DOY)	n.a.	237.00
	Maximum (DOY)	n.a.	250.00
	Minimum (DOY)	n.a.	210.00
	Standard deviation (days)	n.a.	12.69

n.a. means that no reference phenological measurements were available. Flowering for SNM and End of Season for VIN are two stages extremely difficult to obtain through reference observations. For this reason they were not considered in this study

measures. Table 10.3 presents the statistics of reference phenological measures obtained for each study area. For the VIN test site, the reference phenological measures were obtained by field collection, according to the Baggiolini scale (Baggiolini 1952). The bud break (BUB), flowering (FLO) and veraison (VER, define as the 'change of color grapes' stage) reference measurements were compared with the SOS, MAT and SEN derived by PhenoSat. As no ground measures of phenology were available for SNM, the PhenoSat results for SNM were compared with the observed measures (named reference measures from this point) derived by visual inspection of the original VI time-series, taking into account the knowledge of the vegetation behavior in the field at normal conditions. As an example, Fig. 10.6 presents the reference measures determined from the SNM for 1 year. The SOS was determined as the first point where a significant (four or more points) NDVI growth was occurred (March/April). The MVD was identified as the maximum NDVI value in the annual time-series, which generally occurs in June or early July. The abrupt decrease verified after this point is due to the grass cutting process. The remaining ground vegetation (about 5 cm height) begins a senescence period until the maximum senescence (EOS), occurring mostly around August. In general the SNM EOS stage is followed by a regrowth (RG), representing the first significant (three or more points) vegetation growth after the EOS occurrence.

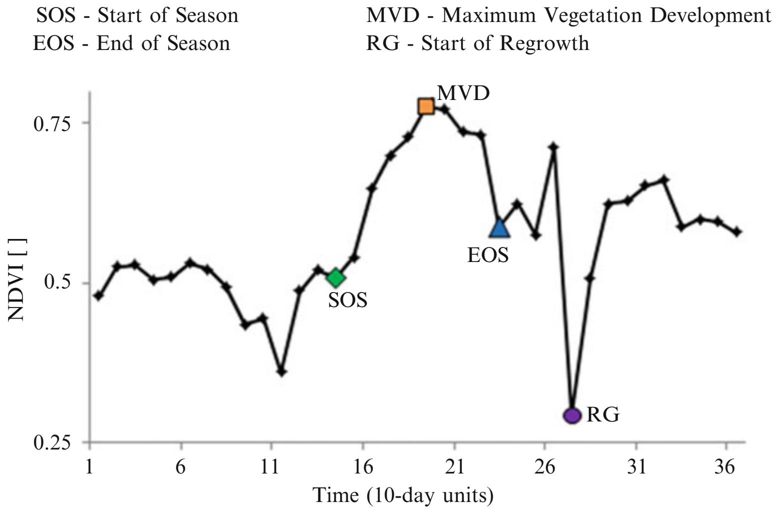

Fig. 10.6 Example of phenological "reference measures" derived from the analysis of a 1-year series (from NDVI SPOT VEGETATION for the semi-natural meadows)

Table 10.4 Correlations between reference and PhenoSat estimated vineyard phenology, using NDVI data from SPOT_VGT and AVHRR sensors

	SPOT_VGT (n = 10)			AVHRR (n = 10)		
Fitting methods	Start	Maturity	Mid-season	Start	Maturity	Mid-season
CSS	−0.27	−0.78	−0.40	0.49	−0.28	0.07
FS	−0.17	−0.76	−0.58	0.56	−0.32	−0.27
GM	0.77	−0.69	0.67	0.45	0.47	0.36
PCF	−0.33	−0.71	−0.38	−0.30	0.41	0.21
PL	0.63	−0.66	−0.55	−0.06	0.30	0.18
SG	0.30	−0.77	−0.25	0.30	−0.21	−0.08

The start, maturity and mid-season represent the comparison between SOSvsBUB, MATvsFLO and SENvsVER, respectively. The SOS, MAT and SEN are the derived PhenoSat phenology, and BUB, FLO and VER are the phenological measures obtained in the vineyard
Fitting methods: *CSS* Cubic Smoothing Splines, *FS* Fourier Series, *GM* Gaussian Models, *PCF* Polynomial Curve Fitting, *PL* Piecewise-Logistic, *SG* Savitzky-Golay

10.4 Results and Discussion

10.4.1 PhenoSat-Derived Phenology

The VIN phenological parameters estimated by PhenoSat were compared with those obtained from reference measurements. The results are presented in Table 10.4.

Using the SPOT_VGT data, the correlations obtained for the start-of-season were no higher than 33 %, except for GM and PL which obtained, respectively, values of 0.77 ($n = 10$; $p = 0.004$) and 0.63 ($n = 10$; $p = 0.025$). The inter-row vegetation growth during the winter, and the difficulty in discriminating the first grapevine leaves from the satellite data, makes it difficult to estimate with high precision the SOS VIN stage. For maturity and mid-season stages, representing the period around VIN full canopy, PhenoSat obtained, in general, higher correlations than for the SOS stage.

The NDVI values for AVHRR were always greater than SPOT_VGT values (Fig. 10.5b), being the higher differences at the end of the years. Comparing with reference measurements (Table 10.4), the AVHRR data achieved better correlations for the SOS, for most of the fitting methods. For the remaining phenological stages, the SPOT_VGT data were better, providing correlations above 70 % ($n = 10$; $p \leq 0.012$), in some cases.

The overall results proved that PhenoSat is capable to extract phenological information from VI data provided by different satellite sensors, with a slightly better performance for the SPOT_VGT. The AVHRR sensor was not originally designed for vegetation studies (Cracknell 1997), having some limitations as water vapor sensitivity and lacks on quality and atmospheric corrections. These limitations are partially solved by the SPOT_VGT sensor that was specifically designed to capture the main characteristics of the vegetation development in the land surface, presenting better navigation, atmospheric correction and improved radiometric sensitivity system (Gobron et al. 2000).

The flexibility of PhenoSat to extract phenology data from different land use types was tested using the SNM. A comparison between the estimations and reference measures is presented in Table 10.5. The phenological dates for SOS, MVD and EOS stages were extracted with a reasonable precision with correlations higher than 0.50 in most cases. All the fitting methods produced similar results, being PCF the method with best performance for the SOS stage ($n = 10$; $r = 0.86$; $p = 0.001$).

Table 10.6 shows the standard error (SE) of PhenoSat estimations obtained using NDVI SPOT_VGT data, for VIN and SNM crops. For VIN, the SE was not

Table 10.5 Comparison between reference and PhenoSat estimated phenology for the semi-natural meadows crop, using SPOT_VGT data

Correlation Reference vs PhenoSat			
Fitting methods	Start of season	Maximum vegetation development	End of season
CSS	0.58	0.54	0.51
FS	0.50	0.45	0.66
GM	0.43	0.56	0.63
PCF	0.86	0.44	0.63
PL	0.38	0.51	0.65
SG	0.53	0.53	0.54

Fitting methods: *CSS* Cubic Smoothing Splines, *FS* Fourier Series, *GM* Gaussian Models, *PCF* Polynomial Curve Fitting, *PL* Piecewise-Logistic, *SG* Savitzky-Golay

Table 10.6 Standard error of PhenoSat estimations using SPOT_VGT data for the two crops studied

	Vineyard			Semi-natural meadows		
Fitting methods	SOS	Maturity	Mid-season	SOS	Maximum vegetation development	EOS
CSS	6.76	4.08	2.22	16.5	14.4	10.2
FS	7.95	4.35	3.21	11.2	14.1	12.3
GM	8.03	5.65	2.44	7.2	14.1	10.7
PCF	9.94	4.08	4.21	13.1	14.3	10.3
PL	5.08	2.47	1.76	11.7	4.4	5.4
SG	8.83	4.08	4.12	15.3	14.9	10.4

SOS Start of season, *EOS* End of season
Fitting methods: *CSS* Cubic Smoothing Splines, *FS* Fourier Series, *GM* Gaussian Models, *PCF* Polynomial Curve Fitting, *PL* Piecewise-Logistic, *SG* Savitzky-Golay

higher than 10 days. The higher values were obtained for VIN SOS stage, being in accordance with the low correlations showed in Table 10.4. For both VIN and SNM crops, the PL was, in general, the best method with a minimum SE for the VIN mid-season of 1.76 days, and a maximum of 11.7 days for SNM start of season.

The capability of PhenoSat in determining multiple growths in a same year was also tested using the SNM data. This crop is characterized by an annual regrowth around the month of August. However, the start of the regrowth can suffer changes due to some factors such as the climatic conditions and human intervention.

Figure 10.7 presents the original and smoothed NDVI SPOT_VGT profiles for the SNM land use type, for the three final years (2008, 2009 and 2010). The smoothed data were obtained using a SG filter with a first degree polynomial and frame size 5. These parameters removed the outliers/spikes without suppressing the natural variations of the SNM VI original data. From the analysis of the smoothed profiles it is possible to see that 2010 is the only year that presents a double growth season, with start (3 or more consecutive points increasing) around the DOY 270. Table 10.7 shows the timing of regrowth derived from the original data and determined using PhenoSat. All six fitting methods were capable to detect the start of the regrowth, obtaining similar results. The similar, and in some cases equal, results can be explained by the fact that the regrowth estimations are obtained using the pre-smoothed data (removed outliers and SG application). These pre-smoothed data present high correlation (around 88 %) with the original data, thus allowing a more realistic analysis and leading to more reliable results. In the years 2001, 2003, 2007, 2008 and 2009 there was no regrowth, which was correctly verified by PhenoSat. For the remaining years, PhenoSat accurately detected the beginning of the double growth season, being the differences between original and estimated parameters of 10-days (except for PCF in the year 2004). Similar conclusions were observed for the maximum of the regrowth.

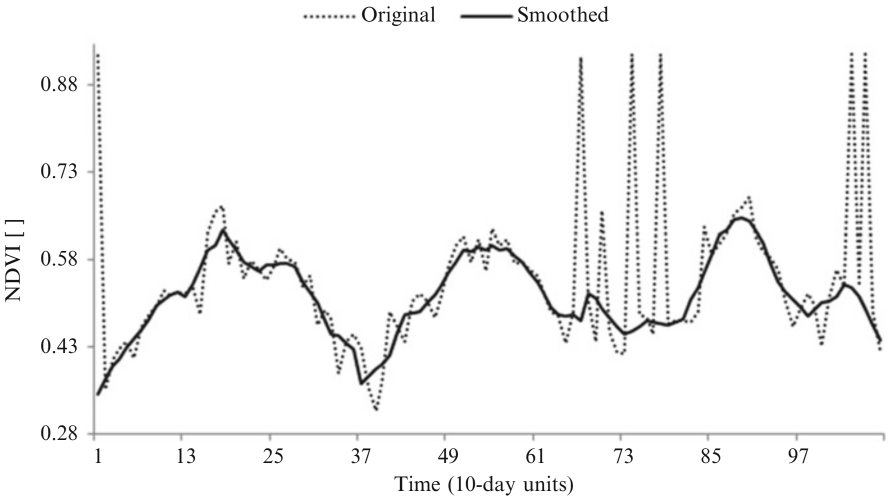

Fig. 10.7 Original and smoothed NDVI SPOT VEGETATION time-series for the semi-natural meadows crop, for years 2008, 2009 and 2010

Table 10.7 Start of double growth season estimations using original and fitted data, for semi-natural meadows

	Start of double growth (day of the year)									
Method	2001	2002	2003	2004	2005	2006	2007	2008	2009	2010
CSS	n.a.	260	n.a.	230	260	250	n.a.	n.a	n.a.	260
FS	n.a.	270	n.a.	230	260	260	n.a.	n.a.	n.a.	260
GM	n.a.	260	n.a.	230	260	260	n.a.	n.a.	n.a.	270
PCF	n.a.	260	n.a.	250	270	260	n.a.	n.a.	n.a.	270
PL	n.a.	260	n.a.	230	260	250	n.a.	n.a.	n.a.	260
SG	n.a.	260	n.a.	230	260	250	n.a.	n.a.	n.a.	280
Original	n.a.	260	n.a.	230	260	250	n.a.	n.a.	n.a.	270

n.a. signifies that no regrowth is verified on this year
Fitting methods: *CSS* Cubic Smoothing Splines, *FS* Fourier Series, *GM* Gaussian Models, *PCF* Polynomial Curve Fitting, *PL* Piecewise-Logistic, *SG* Savitzky-Golay

10.4.2 Advantages of Selecting an In-season Region of Interest

PhenoSat has the option to select a region of interest, instead of using all range of observations in a year. The reduction of the VI time-series improves the fitting process, capturing more efficiently the maximum vegetation development, thus producing more realistic results. To evaluate the utility of this feature on phenological studies, PhenoSat was tested using the VIN. The interest region must be selected according to the behavior of the studied vegetation in the field, under normal conditions. The grape-growth cycle in Douro (Portugal) starts with the bud break stage, which occurs around March. The harvest period typically occurs

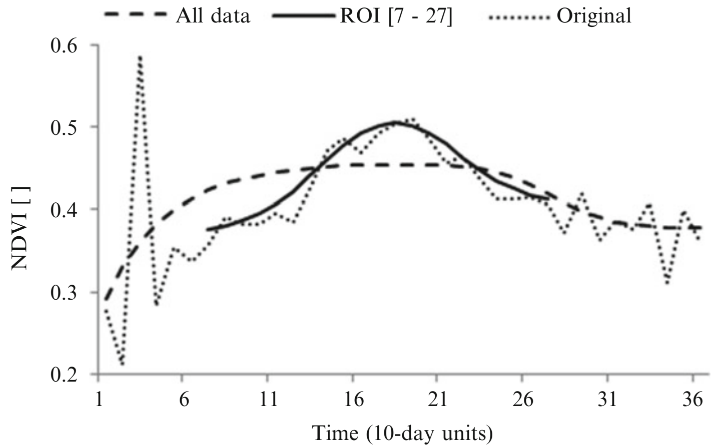

Fig. 10.8 NDVI SPOT VEGETATION original time-series (*dot line*) and the piecewise-logistic fitted results using all range of observations (*dash line*) and the in-seasonregion of interest (*solid line*), for the vineyard in 2009

between August and September/October, however it is deeply dependent on the winemakers according to the style and quality of the wine they wish to produce. Considering these facts, the main phenological cycle of the studied VIN crop is assumed to be ranged from March (DOY 70) to September (DOY 270).

Figure 10.8 presents the VIN NDVI SPOT_VGT data for the year 2009, and the PL fitting results using all range of observations (dash line) and the in-season region of interest. Using all range of observations, the maximum peak of the VIN (around the DOY 180/190) cannot be detected due to the initial peak around the DOY 30 that could be related with winter vegetation growth in the vineyard inter-row. The inclusion of this early pick of NDVI profile led to an over smoothed of the main growing cycle. On the other hand, the use of the region of interest allowed a more accurate adaptation of the fitting method to the variations of the original data during the main growth cycle. The full canopy and senescence stages were captured with high precision and more realistic results were produced. The PL fitted data, produced using region of interest (from 7 to 27 10 days NDVI; 21 observations) instead the all 36 observations, improves the R-square from 0.596 to 0.997.

Another example of the importance of the use of the interest zone in vineyards is presented in Fig. 10.9. The PL fitted results, using all the 36 observations, captured the initial peak (DOY 70) as the maximum development of the VIN crop. This erroneous information led to non-accurate phenological estimations. Using the region of interest, the fitted results captured more precisely the VIN growing season, over smoothing the period related with the soil vegetation growth.

The selection of a region of interest proved to be useful not only in reducing the processing time, but also in obtaining better fitted results, and consequently more reliable phenological information.

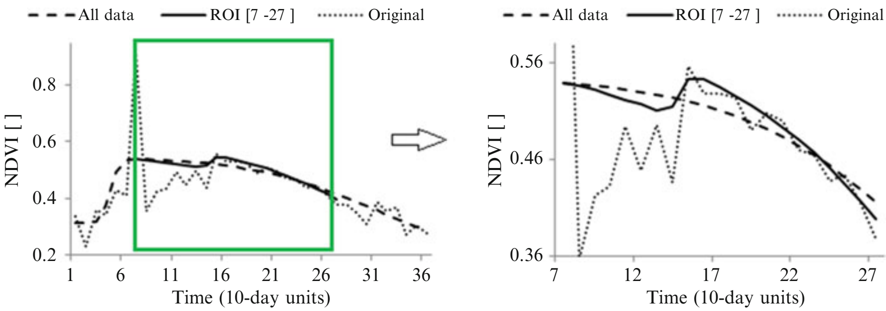

Fig. 10.9 NDVI SPOT VEGETATION original time-series (*dot line*) and the piecewise-logistic fitted results using all range of observations (*dash line*) and using an inseason region of interest (*solid line*), for the vineyard in 2001

10.5 Conclusions

PhenoSat is an easy-to-use software tool which enables phenological information to be extracted from satellite VI data. The experiments carried out indicate that PhenoSat is capable of estimating phenological metrics with significant precision, obtaining, in some cases, correlations with reference measurements above 70 % ($n = 10$; $p \leq 0.012$).

PhenoSat permits the detection of an annual regrowth and the possibility to define an in-season region of interest, which are limitations of other software packages used to extract phenology.

The option to select an in-season region of interest results on an improvement of the fitting process, leading to more reliable results. This PhenoSat feature proved to be a valuable tool for vineyard monitoring and can extend the PhenoSat application to crops with discontinuous canopy, like forestry and deciduous fruit trees. PhenoSat proved to be capable to detect efficiently the regrowth occurrence. The independency of the fitted results leads to a more realistic time-series profile over the year and, thus, more accurate regrowth-derived results.

Comparing PhenoSat with other tools available for phenological studies (e.g. TIMESAT, HANTS, Enhanced TIMESAT, PPET), PhenoSat appears as an intuitive, easy-to-use software with two new important features: the possibility to select an in-season region of interest, and the capability of identifying multiple regrowth within a single year. Moreover, the extraction of phenological parameters using an algorithm based on changes of growth rates allows PhenoSat to avoid thresholds or empirical constants, providing a flexible tool that can be applied to different crops and VI data provided from different data sources.

PhenoSat is freely available at http://www.fc.up.pt/PhenoSat website.

Acknowledgments The authors would like to thank JOINT RESEARCH CENTRE (Community Image Data portal) for providing access to the SPOT_VGT and AVHRR images.

Arlete Rodrigues would like to thank to Fundação para a Ciência e a Tecnologia (FCT) for the Doctoral Grant (SFRH/BD/62189/2009).

Part of this project was supported by European Regional Development Fund (ERDF), programme COMPETE and National funds by FCT – Fundação para a Ciência e a Tecnologia, project PTDC/AGR-AAM/67182/2006, LAMESAT_XXI.

References

Allen WA, Gausman HW, Richardson AJ, Thomas JR (1969) Interaction of isotropic light with a compact plant leaf. J Opt Soc Am 59:1376–1379

Allen WA, Gausman HW, Richardson AJ (1973) Willstater-stoll theory of leaf reflectance evaluated by ray tracing. Appl Opt 12:2448–2453

Atzberger C, Eilers PHC (2010) A smoothed 1-km resolution NDVI time series (1998–2008) for vegetation studies in South America. Int J Digital Earth 4:365–386

Atzberger C, Rembold F (2009) Estimation of inter-annual winter crop area variation and spatial distribution with low resolution NDVI data by using neural networks trained on high resolution images. Proc SPIE Remote Sens Agric Ecosyst Hydrol XI: 7472

Baggiolini M (1952) Les stades repères dans le développement annuel de la vigne et leur utilization pratique. Revroman de Agric Vitic Arboric 8:4–6

Beck PSA, Atzberger C, Hogda KA, Johansen B, Skidmore AK (2006) Improved monitoring of vegetation dynamics at very high latitudes: a new method using MODIS NDVI. Remote Sens Environ 100(3):321–334

Bradley BA, Mustard JF (2008) Comparison of phenology trends by land cover class: a case study in the Great Basin, USA. Glob Chang Biol 14:334–346

Bradley B, Jacob R, Hermance J, Mustard J (2007) A curve fitting procedure to derive inter-annual phenologies from time-series of noisy satellite NDVI data. Remote Sens Environ 106:137–145

Cao R, Chen J, Shen M, Tang Y (2015) An improved logistic method for detecting spring vegetation phenology in grasslands from MODIS EVI time-series data. Agric For Meteorol 200:9–20

Carreiras JMB, Pereira JMC, Shimabukuro YE, Stroppiana D (2003) Evaluation of compositing algorithms over the Brazilian Amazon using SPOT-4 Vegetation data. Int J Remote Sens 24(17):3427–3440

Chen J, Jonsson P, Tamura M, Gu Z, Matsushita B, Eklundh L (2004) A simple method for reconstructing a high-quality NDVI time-series data set based on the Savitzky-Golay filter. Remote Sens Environ 91:332–334

Colditz RR, Conrad C, Wehrmann T, Schmidt M, Dech S (2008) TiSeG: a flexible software tool for time-series generation of MODIS data utilizing the quality assessment science data set. IEEE Trans Geosci Remote Sens 46:3296–3308

Cracknell AP (1997) The advanced very high resolution radiometer. Taylors &Francis Publisher, London. ISBN 0-7484-0209-8

Cunha M, Marcal ARS, Rodrigues A (2010) A comparative study of satellite and ground-based vineyard phenology. In: Proceedings of the 29th symposium on EARSeL, Chania, Greece, pp 68–77

de Beurs KM, Henebry GM (2004) Land surface phenology, climatic variation, and institutional change: analyzing agricultural land cover change in Kazakhstan. Remote Sens Environ 89: 497–509

Eerens H, Haesen D, Rembold F, Urbano F, Tote C, Bydekerke L (2014) Image time series processing for agriculture monitoring. Environ Model Softw 53:154–162

Fontana F, Rixen C, Jonas T, Aberegg G, Wunderle S (2008) Alpine grassland phenology as seen in AVHRR, VEGETATION and MODIS NDVI time series – a comparison with in situ measurements. Sensors 8(4):2833–2853

Gao F, Morisette JT, Wolfe RE, Ederer G, Pedelty J, Masuoka E, Myneni R, Tan B, Nightingale J (2008) An algortithm to produce temporally and spatially continuous MODIS-LAI time series. IEEE Geosci Remote Sens Lett 5:60–64

Gausman HW, Allen WA (1973) Optical parameters of leaves of 30 plant species. Plant Physiol 52:57–62

Gausman HW, Hart WG (1974) Reflectance of sooty mold fungus on citrus leaves over the 2.5 to 40-micrometer wavelenght interval. J Econ Entomol 67:479–480

Gausman HW, Allen WA, Myers VI, Cardenas R (1969) Reflectance and internal structure of cotton leaves Gossypium hirsutum L. Agron J 61:374–376

Gausman HW, Allen WA, Escobar DE (1974) Refractive index of plant cell walls. Appl Opt 13:109–111

Gobron N, Pinty B, Verstraete M, Widlowski J (2000) Development of spectral indices optimized for the VEGETATION instrument. Proc VEGETATION 2000:275–280

Goshtasby A, Oneill WD (1994) Curve-fitting by a sum of Gaussians. CVGIP – Graph Models Image Process 56(4):281–288

Gutman GG (1991) Vegetation indexes from AVHRR – an update and future-prospects. Remote Sens Environ 35(2/3):121–136

Higham DJ, Higham NJ (2000) Matlab guide. SIAM, Philadelphia

Holben BN (2007) Characteristics of maximum-value composite images from temporal AVHRR data. Int J Remote Sens 7(11):1417–1434

Jonsson P, Eklundh L (2002) Seasonality extraction by function fitting to time-series of satellite sensor data. IEEE Trans Geosci Remote Sens 40(8):1824–1832

Jonsson P, Eklundh L (2004) TIMESAT – a program for analyzing time-series of satellite sensor data. Comput Geosci 30(8):833–845

JRC-CID: Joint Research Centre Community Image Data portal (2013) Available at http://cidportal.jrc.ec.europa.eu/home/. Accessed 13 July 2013

Julien Y, Sobrino JA (2009) Global land surface phenology trends from GIMMS database. Int J Remote Sens 30:3495–3513

Lhermitte S, Verbesselt J, Verstraeten WW, Coppin P (2011) A comparison of time series similarity measures for classification and change detection of ecosystem dynamics. Remote Sens Environ 115:3129–3152

Li Z, Kafatos M (2000) Interannual variability of vegetation in United States and its relation to El Nino/Southern Oscillation. Remote Sens Environ 71:239–247

Li XW, Strahler AH (1992) Geometric-optical bidirectional reflectance modeling of the discrete crown vegetation canopy-Effect of crown shape and mutual shadowing. IEEE Trans Geosci Remote Sens 30(2):276–292

Lovell JL, Graetz RD (2001) Filtering pathfinder AVHRR land NDVI data for Australia. Int J Remote Sens 22:2649–2654

Ma M, Veroustraete F (2006) Reconstructing pathfinder AVHRR land NDVI time-series data for the Northwest of China. Adv Space Res 37:835–840

McCloy KR, Lucht W (2004) Comparative evaluation of seasonal patterns in long time series of satellite image data and simulations of global vegetation model. IEEE Trans Geosci Remote Sens 42:140–153

McKellip R, Prados D, Ryan R, Ross K, Spruce J, Gasser G, Greer R (2008) Remote-sensing time series analysis, a vegetation monitoring tool. NASA Tech Briefs 32:63–64

McKellip RD, Ross KW, Spruce JP, Smoot JC, Ryan RE, Gasser GE, Prados DL, Vaughan RD (2010) Phenological parameters estimation tool. NASA Tech Briefs, September 30. New York

Mitra SK (2010) Digital signal processing: a computer-based approach, 4th edn. McGraw-Hill Science/Engineering/Math, Boston. ISBN 978-0077366766

Montgomery D, Peck E, Vining G (2006) Introduction to linear regression analysis, 4th edn. Wiley, Hoboken

Pocas I, Cunha M, Pereira LS (2012) Dynamics of mountain semi-natural grassland meadows inferred from SPOT-VEGETATION and field spectroradiometer data. Int J Remote Sens 33(14):4334–4355

Potter C, Tan PN, Steinbach M, Klooster S, Kumar V, Myneni R, Genovese V (2003) Major disturbance events in terrestrial ecosystems detected using global satellite data sets. Glob Chang Biol 9:1005–1021

Prados D, Ryan RE, Ross KW (2006) Remote sensing time series product tool. AGU Fall Metting 2006

Press WH, Teukolsky SA, Vetterling WT, Flannery BP (2007) Numerical recipes: the art of scientific computing, 3rd edn. Cambridge University Press, Cambridge, pp 766–768. ISBN 10:0521880688

Reinsch CH (1967) Smoothing by spline functions. Numer Math 10:177–183

Rodrigues A, Marcal ARS, Cunha M (2013) Monitoring vegetation dynamics inferred by satellite data using the PhenoSat tool. IEEE Trans Geosci Remote Sens 51(4):2096–2104

Roerink GJ, Menenti M, Verhoef W (2000) Reconstructing cloud free NDVI composites using Fourier analysis of time series. Int J Remote Sens 21(9):1911–1917

Ross KW, Spiering BA, Kalcic MT (2009) Monitoring phenology as indicator for timing of nutrients inputs in northern gulf watersheds. Oceans'09 MTS/IEEE Conference, October 26–29, United States

Sakamoto T, Yokozawa M, Toritani H, Shibayama M, Ishitsuka N, Ohno H (2005) A crop phenology detection method using time-series MODIS data. Remote Sens Environ 96:366–374

Sweets D, Reed B, Rowland J, Marko S (1999) A weighted least-squares approach to temporal smoothing of NDVI. Proc Am Soc Photog Remote Sens Conf 526–536

Tan B, Morisette JT, Wolfe RE, Gao F, Ederer GA, Nightingale J, Pedelty JA (2011) An enhanced TIMESAT algorithm for estimation vegetation phenology metrics from MODIS data. IEEE J Select Top Appl Earth Obs Remote Sens 4(2):361–371

Tucker CJ, Hielkema JU, Roffey J (1985) The potential of satellite remote sensing of ecological conditions for survey and forecasting desert-locust activity. Int J Remote Sens 6(1):127–138

Udelhoven T (2011) TimeStats: a software tool for the retrieval of temporal patterns from global satellite archives. IEEE J Select Top Appl Earth Obs Remote Sens 4(2):310–317

Velleman P (1980) Definition and comparison of robust nonlinear data smoothing algorithms. J Am Stat Assoc 75:609–615

Verbesselt J, Hyndman R, Zeileis A, Culvenor D (2010) Phenological change detection while accounting for abrupt and gradual trends in satellite image time series. Remote Sens Environ 114:2970–2980

Verbesselt J, Jonsson P, Lhermitte S, Jonckheere I, van Aardt J, Coppin P (2012) Relating time-series of meteorological and remote sensing indices to monitor vegetation moisture dynamics. In: Chen CH (ed) Signal and image processing for remote sensing. CRC Press, Boca Raton, pp 129–146

Verschelde J (2007) Introduction to symbolic computation: MCS320. UIC, Dept of Math, Stat & CS, Springer

Viovy N, Arino O, Belward A (1992) The Best Index Slope Extraction (BISE): a method for reducing noise in NDVI time-series. Int J Remote Sens 13:1585–1590

Woolley JT (1971) Reflectance and transmittance of light by leaves. Plant Phisiol 47:656–662

Zeng H, Jia G, Forbes BC (2013) Shifts in Artic phenology in response to climate and anthropogenic factors as detected from multiple satellite time series. Environ Res Lett 8:1–12

Zhang X, Friedl M, Schaaf C, Strahler A, Hodges J, Gao F, Reed F, Huete A (2003) Monitoring vegetation phenology using MODIS. Remote Sens Environ 84:471–475